

F.A. Calderon, R.O. Dendy, S.C. Chapman, A.J. Webster,  
B. Alper, R.M. Nicol and JET EFDA contributors

# Identifying Low Dimensional Dynamics in Type I ELMI Processes in JET Plasmas

“This document is intended for publication in the open literature. It is made available on the understanding that it may not be further circulated and extracts or references may not be published prior to publication of the original when applicable, or without the consent of the Publications Officer, EFDA, Culham Science Centre, Abingdon, Oxon, OX14 3DB, UK.”

“Enquiries about Copyright and reproduction should be addressed to the Publications Officer, EFDA, Culham Science Centre, Abingdon, Oxon, OX14 3DB, UK.”

The contents of this preprint and all other JET EFDA Preprints and Conference Papers are available to view online free at [www.iop.org/Jet](http://www.iop.org/Jet). This site has full search facilities and e-mail alert options. The diagrams contained within the PDFs on this site are hyperlinked from the year 1996 onwards.

# Identifying Low Dimensional Dynamics in Type I ELMing Processes in JET Plasmas

F.A. Calderon<sup>1</sup>, R.O. Dendy<sup>1,2</sup>, S.C. Chapman<sup>1</sup>, A.J. Webster<sup>2</sup>,  
B. Alper<sup>2</sup>, R.M. Nicol<sup>1</sup> and JET EFDA contributors\*

*JET-EFDA, Culham Science Centre, OX14 3DB, Abingdon, UK*

<sup>1</sup>*Centre for Fusion, Space and Astrophysics, Department of Physics,  
University of Warwick, Coventry, CV4 7AL, UK*

<sup>2</sup>*EURATOM/CCFE Fusion Association, Culham Science Centre, Abingdon, OX14 3DB, UK*

*\* See annex of F. Romanelli et al, "Overview of JET Results",  
(23rd IAEA Fusion Energy Conference, Daejeon, Republic of Korea (2010)).*



## ABSTRACT

Edge localised mode (ELM) measurements from reproducibly similar plasmas in the JET tokamak, which differ only in their gas puffing rate, are analysed in terms of the pattern in the sequence of waiting times between successive ELMs. It is found that the category of ELM defined empirically as Type I - typically more regular, less frequent, and having larger amplitude than other ELM types - embraces substantially different ELMing processes. Delay time embedding reveals a transition between distinct phase space structure, implying a transition between distinct underlying physical processes. By quantifying the structure in the sequence of waiting times of ELMs for the first time, we establish a relationship between a control parameter (gas puffing rate) and impulsive events in these nonlinearly coupled multiscale plasmas.

## INTRODUCTION

Enhanced confinement operating regimes (H-mode) in magnetically confined plasmas are accompanied by pulses of energy and particle release known as edge localised modes (ELMs) [1–6]. At steady state, a magnetically confined tokamak plasma comprises a family of nested magnetic flux surfaces in a smooth, or laminar state. ELMing constitutes a relaxation process, for the edge region of H-mode plasmas, which encompasses an initial trigger for linear MHD instability evolving into a fully nonlinear detached state, such that structures propagate to the first wall where they generate recombination radiation. In parallel, local temperature and pressure gradients evolve rapidly. The onset of ELMing accompanies a sharp transition in the global state of the tokamak plasma, and changes in observed ELM character reflect changes in externally applied drive such as gas puffing and heating. Control, mitigation and prediction of the occurrence of large Type I ELMs are central challenges for magnetic confinement fusion plasma physics. There are many active experimental campaigns in this area [7–9], particularly in support of the future ITER tokamak, for which the consequences of uncontrolled Type I ELMs may be unacceptable [4, 6]. While successful theories for some component elements of the ELMing process have been constructed, there is currently no comprehensive first principles model that incorporates all of the physical effects that are known to contribute to the ELMing process. ELM categorisation is primarily phenomenological [3–5], furthermore it is not always easy to discriminate in real time between Type I and, say, Type III ELMing. Hitherto only a few papers [10, 11] have addressed measured ELM sequences as the pulsed outputs of a nonlinear system, a field where generic analysis techniques are well developed and potential links to ELMing have long been apparent [12]. Characterisation of ELMing processes by applying dynamical systems theory to the data offers a fresh avenue to understanding, prediction and control, and may help identify some of the key properties that models for Type I ELMing must embody. Here we take the first steps.

Ruelle and Takens initiated a classical scenario for the transition from ordered to disordered flow in fluids with increasing driving control parameter [14–16]. This has been observed in Rayleigh-Bernard convection in fluids [17–21], and in drift wave turbulence [22] and flute in- stabilities in

plasmas [23]. Underlying the transition is a change in the topology of the phase space trajectory of the system. Oscillatory behaviour arises either if there is a constant of the motion, or if there is a limit cycle onto which the system dynamics is attracted in the presence of damping or dissipation. In the present case, where the system is the plasma undergoing the ELMing process, the nature and number of the relevant phase space co-ordinates is not known from first principles. Progress towards their identification can nevertheless be made by applying techniques of dynamical systems analysis to visualize changes in the topology of the phase space. A convenient method is delay time embedding [24]; one variant of this is to plot the successive time intervals between crossings of a surface of section in the phase space.

In this Letter we report the first application of delay time embedding to the measured time intervals or waiting times between successive ELMs. We consider ELM sequences from six similar plasmas in the JET tokamak, including JET Pulse No:57865 where the H-mode closely approaches an ITER operating regime with respect to some, but not all, key dimensionless parameters [13]. We obtain evidence that Type I ELMing in these plasmas exhibits transitions between processes with distinct physical analogues, dependent on the value of the gas puffing rate as control parameter.

In all six plasmas the toroidal magnetic field density is 2.7T, the plasma current is 2.5MA, neutral beam and ion cyclotron resonance heating power are 13.5MW and 2.0MW respectively, and the  $H_{98}$  confinement factor is in the range 0.87 to 1.0. In all six plasmas, gas puffing terminates at 23.3s and neutral beam heating is ramped down from 23.5 to 24.5s. The differences in Type I ELM character are largely determined by the different levels of externally applied gas puffing. The intensity of the  $D_\alpha$  signal, which sometimes saturates, is not necessarily a reliable proxy for the magnitude of the underlying ELM plasma phenomenon, whereas occurrence times are well defined. ELM occurrence and ELM waiting times are the primary physical indicators addressed in the present study. The moment of occurrence of each ELM is inferred from the  $D_\alpha$  datasets using an algorithm similar to that described in [11], which exploits the steep leading edge of each ELM. This procedure generates a sequence of event times  $t_n$  for each  $n$ th ELM, and hence inter event times  $\delta t_n = t_n - t_{n-1}$ . These sequences are used to construct delay plots; these are known [24] to capture aspects of the topology of the unknown underlying phase space evolution of the system.

Figures 1 and 2 show measured Type I ELM signals for a sequence of six JET H-mode plasmas 578nm, where nm is 72, 71, 70, 65, 67, and 69 in order of increasing magnitude and duration of the gas puffing rate, shown in Fig.3, which is the key external control parameter. The upper trace in each panel of Figs.1 and 2 plots the time-evolving intensity of Lyman alpha recombination radiation from deuterium,  $D_\alpha$ , measured by a camera directed at the inner divertor, normalised by the mean measured intensity. The two groupings of three plasmas are at lower (Fig.1) and higher (Fig.2) gas puffing rates. At lower gas puffing rates (Fig.1) the ELM signal intensity is roughly the same across each time series, whereas at higher gas puffing rates (Fig.2) this shows a rich structure. We will investigate this structure by sorting the ELM events that are used to construct the time series of delays, or waiting times, in terms of whether they exceed a threshold in signal intensity;

the thresholds used are indicated by horizontal lines on the ELM time series (top panel in Figs 1 and 2). Each  $n$ th Type I ELM that has signal intensity exceeding a given threshold then forms a set of events at time  $t_n$  with waiting time, or delay, between events  $\delta t_n = t_n - t_{n-1}$ . The middle panels of Figs.1 and 2 show the delay plots for a given threshold, that is,  $\delta t_{n+1}$  versus  $t_n$ . The  $D_\alpha$  signal intensity for the ELM at  $t_n$  is indicated by colour coding. These delay, or  $n = 1$  embedding, plots reflect the topology of the system phase space. For a trajectory that is approximately singly periodic with period  $t_n$ , the delay plot will exhibit a concentration of points on the  $\delta t_{n+1} = \delta t_n$  line, centred on the mean period. The spread of points about the mean period reflects a combination, in unknown proportions, of intrinsic and extrinsic sources of irregularity in a quasi-regular process, and determines the practical resolution limit of this method. A period-two oscillation will generate two concentrations of points, symmetrically placed either side of the  $\delta t_{n+1} = \delta t_n$  line, whereas dynamical switching between one period  $t_n$  and another at  $\delta t'_n$  will generate four concentrations of points: at the two distinct periods  $\delta t_n$  and  $\delta t'_n$  on the  $\delta t_{n+1} = \delta t_n$  line, and at two symmetrically placed either side of the line, at  $(\delta t_{n+1}, \delta t'_n)$  and  $(\delta t'_{n+1}, t_n)$ .

The delay plots in Fig. 1 are insensitive to the threshold, in marked contrast to Fig.2, suggesting that these reflect distinct processes. In Fig.1, plasmas with successively greater gas puffing rates are shown left to right. We can see that increased gas puffing causes the ELMing process to bifurcate from singly periodic (Pulse No: 57872), via transitional behaviour (Pulse No: 57871), to a situation where two periods are present (Pulse No: 57870) together, with the plasma switching between them. This behaviour is approximately analogous to that of small amplitude oscillations of two weakly coupled pendulums with different natural frequencies. It is also apparent that a longer waiting time  $t_n$  before an ELM correlates statistically with a larger  $D_\alpha$  signal intensity. The bottom pair of plots in each panel of Figs.1 and 2 displays the probability density functions (pdfs) for the distributions of measured  $t_n$  for the ELM time series using the same amplitude thresholds as for the delay plots; in Fig.1, unlike Fig.2, these two panels are identical.

We now turn to Fig.2 which corresponds to higher overall levels of gas puffing rate. It displays a transition in the ELMing process as the gas puffing rate is increased, which is different to that seen in Fig.1. Each ELM with large  $D_\alpha$  signal intensity is statistically likely to be rapidly followed by a population of postcursor ELMs with smaller  $D_\alpha$  signal intensity. The likelihood of a postcursor ELM, and their number, increases with gas puffing rate. As a consequence, the delay plots constructed for different thresholds now, unlike Fig.1, show different structure. At relatively low gas puffing rate (left hand plots) most delays fall within a single group on the  $\delta t_{n+1}, \delta t_n$  line. However when the threshold is reduced, smaller postcursor events begin to feature in the time series of delays and result in populations (lines parallel to the axes) far from the  $\delta t_{n+1}, \delta t_n$  line, and a new, narrowly constrained group on the  $\delta t_{n+1}, \delta t_n$  line at small  $(\delta t_{n+1}, \delta t_n)$ . As the gas puffing rate is increased, these small postcursor events come to dominate numerically. It is noteworthy that whereas there is a broad distribution of waiting times between successive ELMs with large signal amplitude, the waiting time between successive postcursor ELMs is very sharply defined and is invariant between

the three JET plasmas. Its inverse defines a potentially important natural frequency of the ELMing process. This process, as seen in the delay plots, is analogous to random large amplitude transient impulses driving a system that has a narrowband resonant frequency response.

Figure 3 displays the gas puffing rates for all six JET plasmas. The clear changes in ELMing displayed in Fig.1, and for JET Pulse No's: 57867 to 57869, arise under comparatively small changes in gas puffing, while there is a relative large step (a factor of approximately two) between JET Pulse No's: 57865 and 57867. Other ELM interval dynamics are in principle possible for other gas fuelling rates, especially for fuelling rates between those of JET Pulse No's: 57865 and 57867, for these otherwise identical plasma operating regimes.

These results represent the first identification and characterization of ELMing transitions by analysis of the time series of inter-ELM time intervals. We have exploited the similarity of these six JET plasmas which all have exceptionally long duration  $\approx 5$ s of the quasi-stationary ELMing process, and which appear to have only one effective control parameter, the gas puffing rate. These particular experiments yield a sufficient number of ELMs and ELM waiting times, to enable us to begin to apply some of the classic techniques of modern nonlinear time series analysis.

This has revealed that transitions in the underlying dynamics are captured in these datasets. It is remarkable that such clearly defined transitions appear to be identifiable given only a few hundred ELM events per plasma, together with the degree of dispersion visible for period one. The identification of detailed dynamical phase space structure from delay plots is challenging in any macroscopic system. Confirmation of its occurrence in JET fusion plasmas would point to a correspondence between ELM physics and a wider class of nonlinear phenomena in fluids. Our results further suggest that the ELMing processes in these plasmas are describable in terms of low dimensional dynamics, notwithstanding the many degrees of freedom that play a part in ELMing from both first principles and empirical perspectives. If confirmed and found more widely, this would inform the construction of future models for ELMing, and could assist ELM mitigation and control. This work indicates that application of dynamical systems techniques and concepts to more extensive ELM datasets would be fruitful.

#### **ACKNOWLEDGMENTS:**

This work, supported by the European Communities under the contract of Association between EURATOM and CCFE, was carried out within the framework of the European Fusion Development Agreement. The views and opinions expressed herein do not necessarily reflect those of the European Commission. This work was also part-funded by the RCUK Energy Programme under grant EP/I501045. We acknowledge the UK EPSRC for support.

#### **REFERENCES**

- [1]. Keilhacker M, Plasma Physics and Controlled Fusion, **26**, 49 (1984)
- [2]. Erckmann V, et al, Physical Review Letters, **70**, 2086 (1993)

- [3]. Zohm H, Plasma Physics and Controlled Fusion, **38**, 105 (1996)
- [4]. Loarte A. et al, Plasma Physics and Controlled Fusion, **45**, 1549 (2003)
- [5]. Kamiya K. et al, Plasma Physics and Controlled Fusion, **49**, S43 (2007)
- [6]. Hawryluk, R. et al., Nuclear Fusion, **49**, 065012, (2009)
- [7]. Evans T. et al, Nature Physics, **2**, 419 (2006)
- [8]. Liang Y. et al, Physical Review Letters, **98**, 265004 (2007)
- [9]. Kirk A. et al, Phys. Physical Review Letters, **108**, 255003 (2012)
- [10]. Degeling A. et al, Plasma Physics and Controlled Fusion, **43**, 1671 (2001)
- [11]. Greenough J. et al, Plasma Physics and Controlled Fusion, **45**, 747 (2003)
- [12]. Itoh S-I. et al, Physical Review Letters, **67**, 2485 (1991)
- [13]. Pamela J., Ongena J. and JET EFDA Contributions, Nuclear Fusion, **45**, 563 (2005)
- [14]. Ruelle D. and Takens F., Communications in Mathematical Physics, **20**, 167 (1971)
- [15]. Newhouse S, Ruelle, D and Takens F, Communications in Mathematical Physics, **64**, 35 (1978)
- [16]. Trefethen L, Trefethen A, Reddy S, and Driscoll T, Science, **261**, 578 (1993)
- [17]. Bodenschatz E, Pesch W, and Ahlers G, Annual Review of Fluid Mechanics, **32**, 709 (2000)
- [18]. Ahlers G, Physical Review Letters, **33**, 1185 (1974)
- [19]. Gollub J.P. and Swinney H.L, Physical Review Letters, **35**, 927 (1975)
- [20]. Gollub J.P. and Benson S.V, Journal of Fluid Mechanics, **100**, 449 (1980)
- [21]. Libchaber A, Fauve S, and Laroche C, Physica (Amsterdam) 7D, **73** (1983)
- [22]. Klinger T, Latten A, Piel A, Bonhomme G, Pierre T, Dudok de Wit T, Physical Review Letters, **79**, 3913, (1997)
- [23]. Brochard F, Gravier E, Bonhomme G, Physical Review E, **73**, 036403 (2006)
- [24]. Packard, N. H., J. P. Crutchfield, J. D. Farmer, R. S. Shaw, Physical Review Letters, **45**, 712, (1980)

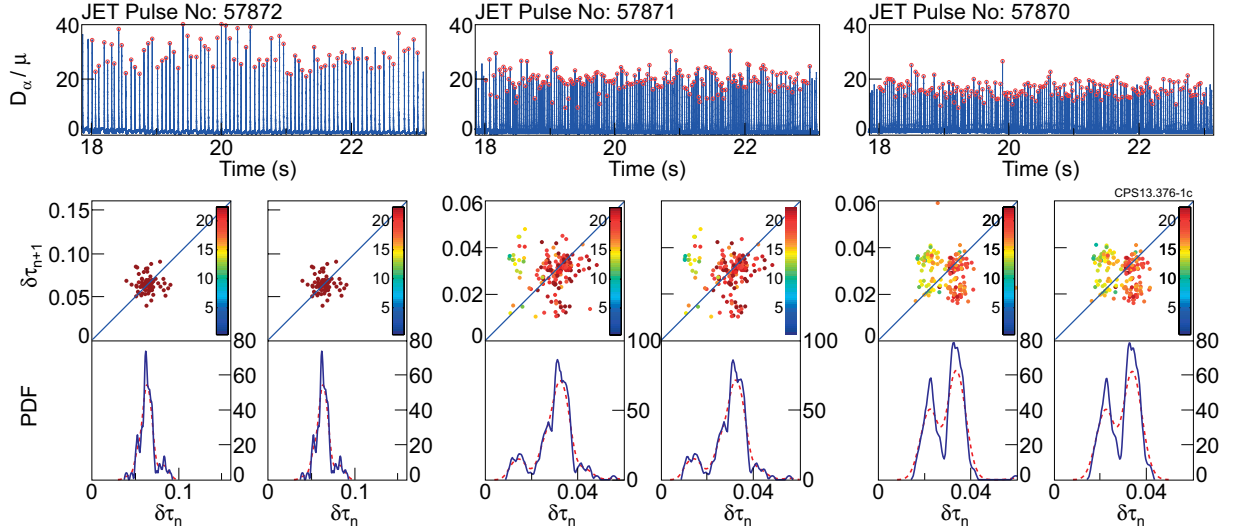


Figure 1: ELM characteristics of three similar JET Pulse No's: 57872, 57871, 57870 at lower gas puffing rates, showing for each plasma: (top of each panel) the time trace of  $D_{\alpha}$  signal intensity, displaying also the two amplitude thresholds used for the centre and bottom plots; (centre of each panel) delay time plots for ELMs, with amplitude colour coded above the higher (lower) threshold on the left (right); (bottom of each panel) corresponding probability density functions for the distributions of measured  $\tau_n$  for the ELM time series, using the same amplitude thresholds as for the delay plots; the red and blue curves represent different binning of the same data. The three plasmas are ordered, from the left, in terms of increasing magnitude of gas puffing, see Fig.3.

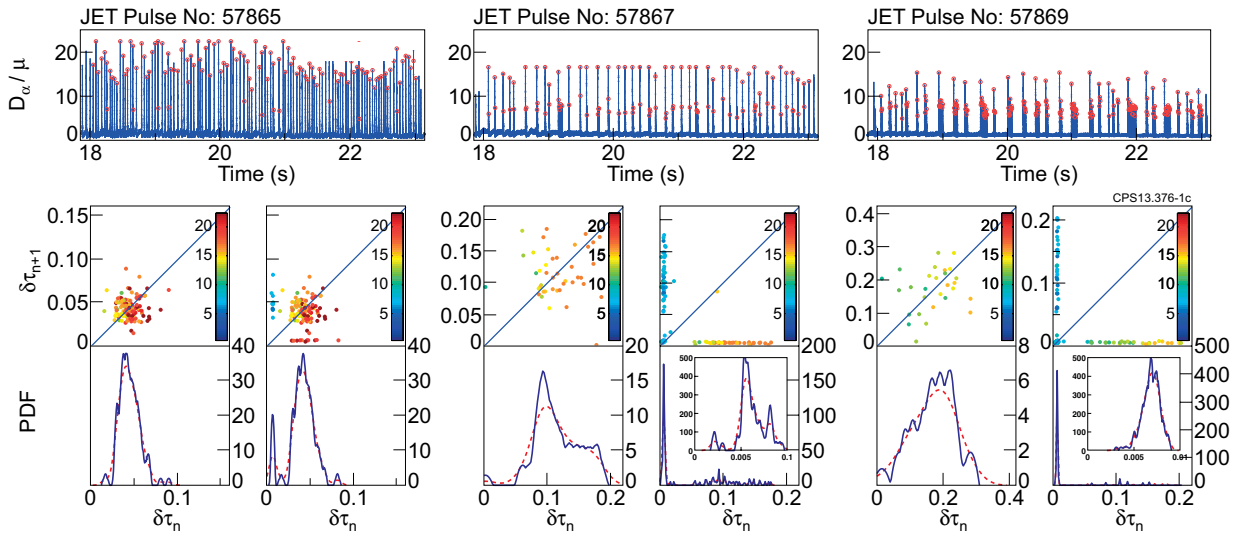


Figure 2: As Fig.1, for three similar JET Pulse No's: 57865, 57867, 57869 at higher gas puffing rates. The three plasmas are ordered, from the left, in terms of increasing magnitude of gas puffing, see Fig.3.

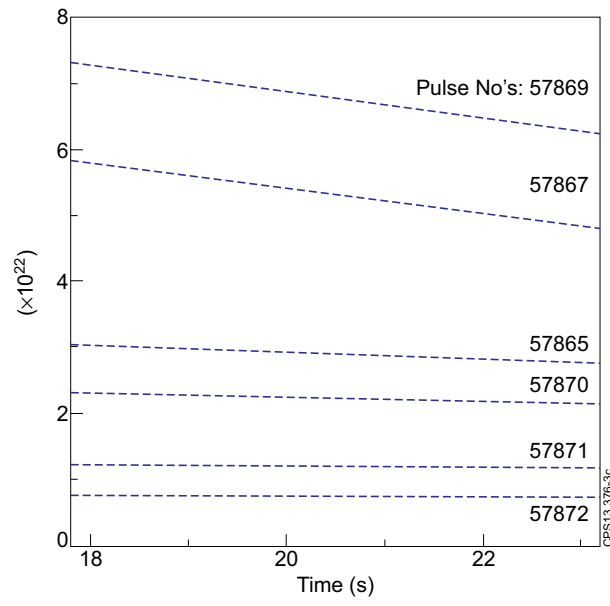


Figure 3: Time trace of gas puffing rate in particles per second, which is the primary external control parameter for the six otherwise similar JET plasmas: ordered, from the bottom, in terms of increasing magnitude.